Radial compression and inward transport of positron plasmas using a rotating electric field*

R. G. Greaves†
First Point Scientific, Inc., 5330 Derry Avenue, Suite J, Agoura Hills, California 91301

C. M. Surko
Department of Physics, University of California, San Diego, California 92093-0319

(Received 30 October 2000; accepted 27 November 2000)

It has recently been demonstrated that positron plasmas confined in a Penning-Malmberg trap can be compressed radially by applying a rotating electric field [Phys. Rev. Lett. **85**, 1883 (2000)]. A more complete description of the original experiments is presented, together with the results of new measurements. Good coupling of the rotating electric field is observed over a broad range of frequencies. The heating caused by the rotating field is counteracted by cooling using a polyatomic gas. Rapid compression rates $\dot{n}/n \sim 15\ s^{-1}$ can be achieved, with central density increases of a factor of 20 or more. The good coupling and high compression rates can be explained in terms of excitation of heavily damped Trivelpiece–Gould modes, or alternatively as coupling directly to particle bounce resonances. Potential improvements and applications are discussed, including the production of high-density positron plasmas and brightness-enhanced positron beams. © *2001 American Institute of Physics.* [DOI: 10.1063/1.1350570]

I. INTRODUCTION

The availability of efficient low-energy positron sources are important in areas as diverse as atomic physics,[1] materials and surface science,[2,3] plasma physics,[4] mass spectrometry,[5] and astrophysical simulations.[6] The development of techniques to accumulate positrons in Penning traps has extended many of these applications and led to new ones.[7] A recent application of positron trapping has been the extraction of high quality pulsed beams with energy spreads as low as 18 meV.[8] Sympathetic cooling of positrons using laser-cooled ions has the potential to produce much colder (i.e., sub-kelvin) plasmas and beams.[9]

The use of Penning traps for the production of positron beams offers unique advantages over conventional positron beam lines. One example is the potential for brightness enhancement by compression of the positron plasma prior to beam extraction, which we recently demonstrated[10] and describe in more detail in this paper. This technique and other capabilities of Penning trap based positron beams (such as the ability to produce ultrashort positron pulses) are currently being developed for the production of bright cold positron beams for a variety of technological applications.[11] Another unique capability is the potential for producing intense positron pulses that can be used, for example, to study Bose-Einstein condensation of positronium atoms[12] or for measurements of anomalous transport in tokamak plasmas.[13]

The ability to compress positron plasmas also has implications for the long-term storage of antimatter, the creation of high density positron plasmas for electron–positron plasma experiments,[4] antihydrogen formation,[14] and the cooling of highly charged ions.[15] The ability to induce inward transport in plasmas is also of relevance in understanding how waves and electric fields alter the transport properties of magnetized plasmas. These types of processes are believed to dominate anomalous transport in magnetically confined neutral plasmas.[16] The ability to study these processes in the unusually simple geometry of the single component plasma has the potential for yielding new understanding of such phenomena.[17]

Several methods have been demonstrated for compressing non-neutral plasmas in the Penning geometry. One method involves varying the plasma rotation frequency using radiation pressure from laser beams.[18] Unfortunately, this technique is restricted to certain species of ion plasmas with suitable electronic transitions. Another method that can be applied more generally to many types of non-neutral plasmas, including those composed of elementary particles, is the injection of angular momentum into the plasma.

Injection of angular momentum has already been demonstrated as a method for compression of both pure electron and pure ion plasmas.[19–23] The angular momentum is injected by applying a rotating electric field (''rotating wall'') to the plasma. In ion plasmas, the signal was applied at a frequency slightly above the $\mathbf{E}\times\mathbf{B}$ rotation frequency of the plasma.[19] For crystallized ion plasmas, the rotation frequency can be phase locked to the applied frequency.[20] In electron plasmas, the frequencies employed are somewhat above the rotation frequency. Maximal plasma compression was obtained when the applied frequencies coincided with those of rotating Trivelpiece–Gould (TG) modes.[21–23]

We note that the technique called magnetron sideband cooling, that is used to shrink the orbits of small collections of particles in harmonic potential traps, is not suitable for use in plasmas. The failure of this technique in plasmas results from the detuning of the characteristic trap resonances due to the significant space charge created by the accumulation of large numbers of particles in a trap.[24]

*Paper MI2 3, Bull. Am. Phys. Soc. **45**, 216 (2000).
†Invited speaker.

In the case of both electron and ion plasmas, the heating produced by the applied rotating electric field must be counteracted by applying some form of strong cooling to the plasma. Both laser cooling and neutral gas cooling have been employed in ion plasma experiments.

Early electron plasma experiments demonstrated the ability to produce inward transport by a rotating field, but no cooling mechanism was present and so only modest compression was achieved.[25] Another experiment utilized the heating from the applied electric field to replenish the plasma by ionization.[26]

More recent electron plasma experiments were conducted in the strong magnetic field of a superconducting magnet,[21,27] where significant cooling is provided by cyclotron radiation from the strongly magnetized particles. This approach can also be employed for compressing positron plasmas for various applications. A positron trap utilizing a superconducting magnet for this purpose is now being constructed at the University of California, San Diego.[28]

For many positron applications, however, it is desirable to avoid a strong magnetic field, especially if the particles must be extracted into the electrostatic beam lines that are typically used for materials science studies and some types of atomic physics experiments. Unfortunately, in a low magnetic field cyclotron cooling is too slow ($\sim$400 s at 1 kG), and so an alternative mechanism must be used.

Recently, we showed for the first time that compression of positron plasmas in low magnetic fields can be achieved using a neutral buffer gas to provide the required cooling.[10] The compression rates observed are about 30 times larger than in earlier electron plasma experiments, thus facilitating the creation of high-throughput positron beam systems. Furthermore, the compression is broadband in character, thus simplifying their practical implementation. Thus, in addition to exploring a new and interesting regime of rotating wall confinement, these results provide a sound scientific basis for the production of high throughput brightness-enhanced positron beams for a variety of technological applications. In this paper, we present additional results and a more complete discussion of the original positron compression experiments. The remainder of this paper is structured as follows. In Sec. II we describe the experimental arrangement and procedures. The experimental results are presented in Sec. III and discussed in Sec. IV, while Sec. V summarizes the paper.

II. EXPERIMENT

Positrons for the experiment were obtained from a three-stage positron accumulator that employs a buffer gas to capture positrons emitted from a radioactive source. The operation and performance of the accumulator are described in detail in Refs. 29 and 30.

The compression experiments were performed in a separate cylindrical Penning-Malmberg trap consisting of 10 cylindrical electrodes of length 3.8 cm and inner diameter 2.54 cm. Six of these electrodes are used to transfer positrons from the accumulator, while the remaining four electrodes formed the compression stage and are illustrated in Fig. 1.

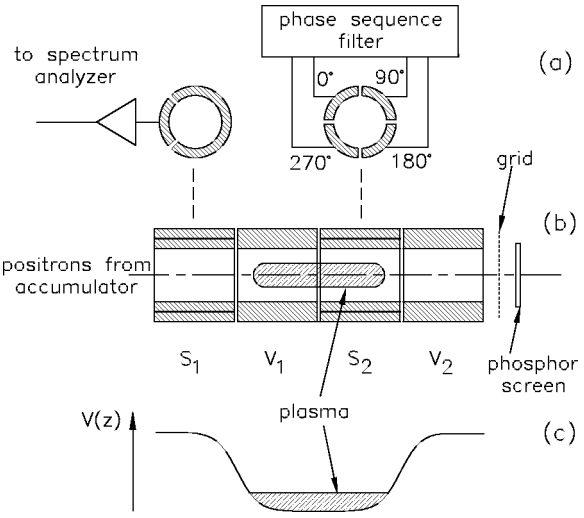

FIG. 1. (a) Electrical connections to segmented electrodes; (b) layout of the positron trap used for compression experiments; and (c) the axial potential well.

Electrode S_2 is azimuthally segmented to allow the application an $m_\theta = 1$ azimuthal perturbation, and S_1 is segmented as shown in Fig. 1 to measure oscillations excited in the plasma. The excitation field consisted of four sine waves of amplitude A_w and frequency f_w, with relative phases shifted by 90° by a broad band phase shifter (0.1–4 MHz). The trap is housed in a vacuum chamber pumped to a base pressure $\sim 1\times10^{-9}$ torr. The radial profiles of the plasma are measured by dumping the positrons from the trap onto a phosphor screen biased to -8 kV and imaging the screen using a charge coupled device (CCD) camera.

Typical parameters before compression were magnetic field, $B = 900$ gauss, plasma radius, $R_p = 3.3$ mm, plasma length, $L_p = 5.5$ cm, number of positrons $N_{\rm tot} = 1\times10^7$, average positron density $n_0 = 5\times10^6$ cm^{-3}, rotation frequency, $\omega_r/2\pi = 50$ kHz, plasma frequency, $\omega_p/2\pi = 20$ MHz, plasma temperature, $k_B T_p = 0.025$ eV and Debye length, $\lambda_D = 0.5$ mm. From these parameters, it can be seen that $\lambda_D \ll L_p, R_p$ and $n_0\lambda_D^3 \sim 10^3 \gg 1$, so the positron cloud is in a well-defined plasma state. In the compressed state, $R_p \simeq 0.7$ mm yielding $n_0 = 8\times10^7$ cm^{-3}.

III. RESULTS

Strong cooling has been found to be crucial for efficient plasma compression using the rotating electric field technique. The ideal cooling gas for positrons should have a low annihilation cross section, large cross sections for inelastic processes such as vibrational and rotational excitation, and a low elastic collision cross section to avoid enhancing cross-field transport. The positron annihilation rates at room temperature are known for a variety of molecules.[31] On the other hand, very little is presently known about elastic and inelastic positron-molecule collision cross sections in the energy regime of interest (i.e., <1 eV), although this energy regime is now being explored using cold positron beams.[32] On the basis of the above criteria, and by considering known electron cross sections that can be expected to give some indica-

TABLE I. Parameters for cooling gases at 2×10^{-8} torr: annihilation time, τ_a (from Ref. 31), measured cooling time; τ_c, vibrational quanta, E_ν, relevant to the cooling; and the maximum measured compression rate $\dot{n}/n_{\max}$.

Gas	$\tau_a(s)$	$\tau_c(s)$	E_ν (eV)	$\dot{n}/n_{\max}$ (s^{-1})
SF_6	2190	0.36	0.076, 0.188	10
CF_4	3500	1.2	0.157	10
CO_2	3500	1.3	0.291, 0.083	4
CO	2400	2.1	0.266	<0.2
N_2	6300	115	0.292 eV	<0.2

tion of the corresponding cross sections for positrons, the following gases were studied: N_2, CF_4, SF_6, CO_2, and CO.

Cooling rates were measured by filling the third stage of the accumulator for a time that is short compared to cooling times of the respective gases ($\sim$10 ms) and then releasing the positrons from the trap after a variable delay. When initially trapped, positrons have a residual energy of several electron volts from the injection process. The positrons cool to room temperature by vibrational and rotational collisions with gas molecules. By measuring the number of positrons released from the trap as a function of the exit gate potential, the positron temperature can be obtained.[33] Using this technique, the cooling times were measured for the selected gases. The results are presented in Table I, together with other parameters relevant to this experiment. These data indicate that cooling times comparable to those of cyclotron radiation cooled plasmas in the field of a superconducting magnet can be obtained using gas cooling at pressures as low as 2×10^{-8} torr. At these pressures positron annihilation on the cooling gas molecules is negligible.

For the compression experiments described here, positrons were transferred from the positron accumulator to the compression trap. The transfer was accomplished in two phases. First, positrons were transferred to the six-segment catching trap mentioned above, by releasing positrons from the accumulator and passing them through the catching trap, while at the same time reducing the depth of the potential well in the catching trap. By carefully tuning the electrode potential so that minimal energy loss was required to trap the positrons in the catching trap, transfer efficiencies of up to 88% were obtained. Positrons were then transferred to the compression trap by further manipulation of the electrode voltages. This two-stage transfer procedure was necessitated by the fact that the potentials of the compression trap electrodes could not be switched on the fast time scales required for positron transfer. This was due to the presence of capacitively coupled electronic components on the compression trap electrodes.

Compression was studied by applying a fixed or swept frequency to electrode S_2 and then dumping the plasma onto the phosphor screen. Typical compression data are presented in Fig. 2. These data show rapid inward transport that begins immediately after the application of the compression field. Because the inward radial transport is rapid, the plasma does not evolve to an equilibrium profile while this transport is occurring, but rather, it develops a dense core which grows

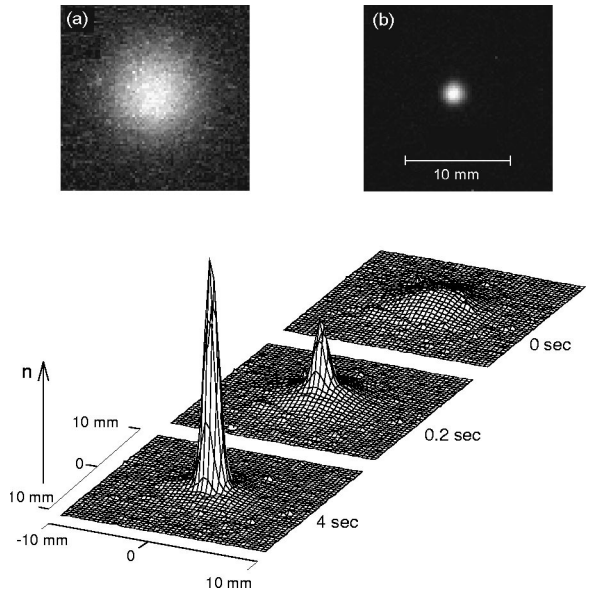

FIG. 2. (a) and (b) CCD images of positron plasmas at $t=0$ and $t=4$ s, respectively. (c) Radial profiles of a positron plasma with $N_{\rm tot}=10^7$ positrons, $f_w=2.5$ MHz, $A_w=56$ mV, and 2×10^{-8} torr of CF_4.

in time as the surrounding plasma is driven inward. There is very little positron loss ($<5\%$) during compression.

Figure 3 shows the time dependence of the central plasma density for different amplitudes of the applied signal. If no signal is applied, the central density decays with an exponential time constant $\sim$11 s. If even a small rotating electric field is applied ($\sim$2 mV), this outward diffusion is reversed, and for larger amplitudes, strong inward transport is obtained. Initially there is an approximately linear increase of density in time, followed by a nonlinear phase and eventual saturation. The minimum radius does not show a strong dependence on the number of positrons in the trap. The smallest radius that was observed was $R_p\simeq0.7$ mm, with a

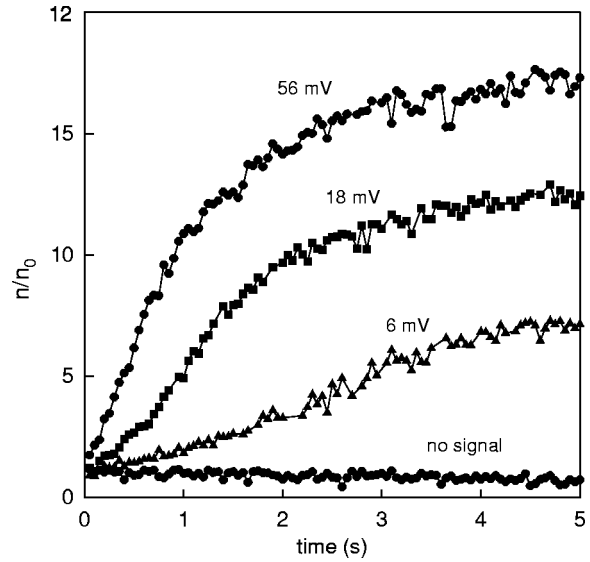

FIG. 3. Time evolution of the central density, n, of a positron plasma normalized to its initial value, n_0, for various values of the applied amplitude; $N_{\rm tot}=10^7$ positrons, $f_w=2.5$ MHz, and 2×10^{-8} torr of CF_4.

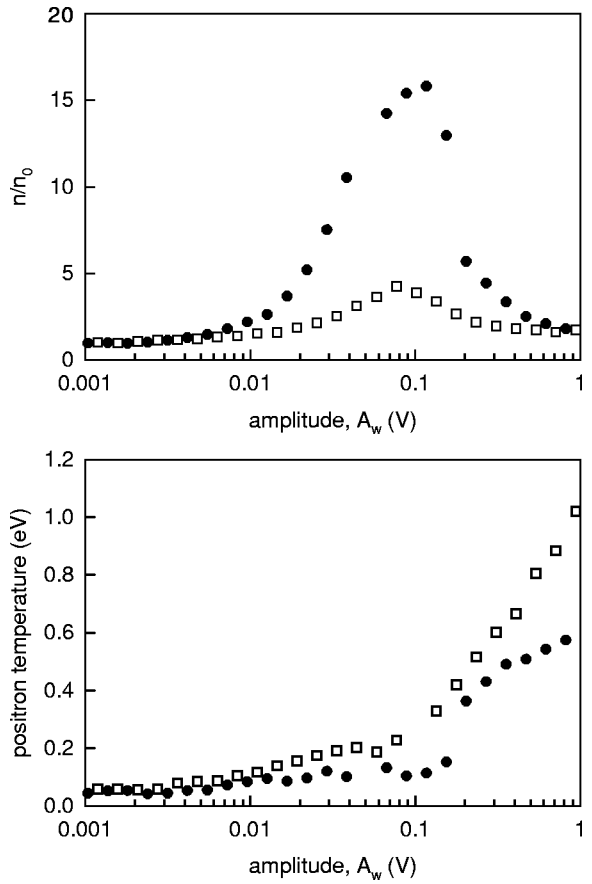

FIG. 4. Dependence of (a) central density and (b) positron temperature with cooling on CF_4 at (●) $P=2.7\times10^{-8}$ torr and (○) $P=6\times10^{-9}$ torr. $f_w=2.5$ MHz for 1 s.

corresponding increase of 20 in central density. Factors determining the minimum radius are not understood at present. A small $m_\theta=1$ diocotron mode is observed to grow as the plasma is compressed, and this may play a determining role in limiting the compression in the present experiment. The observed compression rates are about a factor of 30 larger than those reported in the experiment of Anderegg *et al.*[21]

Figure 4 shows the dependence of the positron temperature on the amplitude of the applied signal for two pressures of the cooling gas. The temperature was measured by measuring the number of particles released from the trap as a function of the exit gate potential.[33] In both cases shown, the positron temperature remains relatively low up to the amplitude where the compression begins to fall off. The failure of compression at the higher amplitudes is therefore clearly related to the loss of cooling. For the data shown in Fig. 4, increasing pressure had the effect of both increasing the degree of compression that can be obtained at a given amplitude, and also of increasing the amplitude at which the compression begins to fail.

Figure 5 shows data for the dependence of compression on the frequency of the applied signal. The data in Fig. 5 were obtained with frequencies in the range 0.1–4 MHz and $A_w=56$ mV applied for 1 s. The central density is normalized to the initial value. For comparison with earlier experiments, we calculated the mode frequencies for the lowest

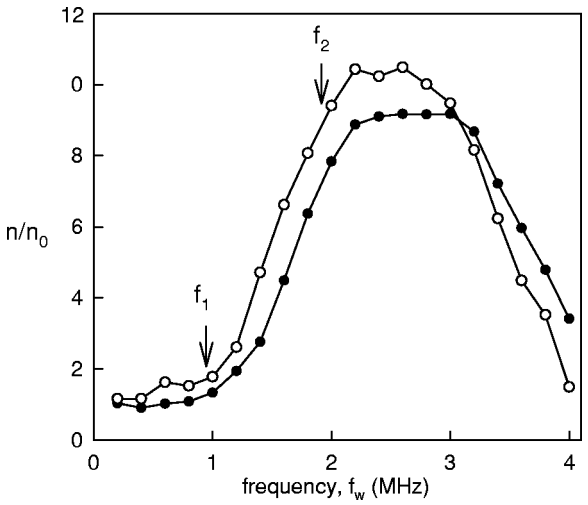

FIG. 5. Dependence of positron density on applied frequency after 1 s of compression for (○) $N_{tot}=1\times10^7$ positrons and (●) $N_{tot}=5\times10^6$ positrons with 2×10^{-8} torr CF_4, $A_w=56$ mV. Arrows indicate the frequencies of the lowest order TG modes for the initial plasma conditions.

order TG modes. In the relevant limit, $kR_p\ll1$, the dispersion relation for the TG modes with $m_\theta=1$ and radial mode number l is

$$\omega\simeq\omega_r\pm kR_p\frac{\omega_p}{p_l}, \tag{1}$$

where p_l is the lth root of $J_1(x)=0$.[22] The frequencies f_1 and f_2 of the two lowest order modes with $m_z=1$ and $m_z=2$, respectively, are indicated by arrows in Fig. 5. It can be seen that compression is observed for frequencies in the range of these low-order TG modes. It is interesting to note, however, that the effect is broad band in character in contrast to the sharp resonances reported in Ref. 21. Attempts to directly detect the excitation of plasma modes using the pickup electrode failed.

In Fig. 6 data are presented for compression as a function of the amplitude of the applied signal. The quantity $\Delta n/n_0$ is plotted, where Δn is the increment in central density after 1 s and n_0 is the initial value. At lower amplitudes,

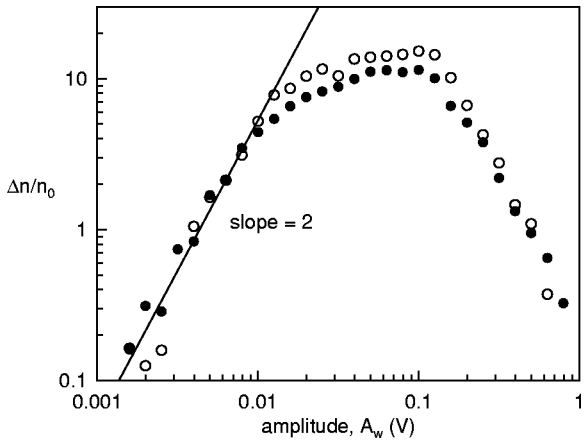

FIG. 6. Positron density on amplitude of applied signal after 1 s of compression for (○) $N_{tot}=1\times10^7$ positrons and (●) $N_{tot}=5\times10^6$ positrons with 2×10^{-8} torr CF_4 and $f_w=2.5$ MHz.

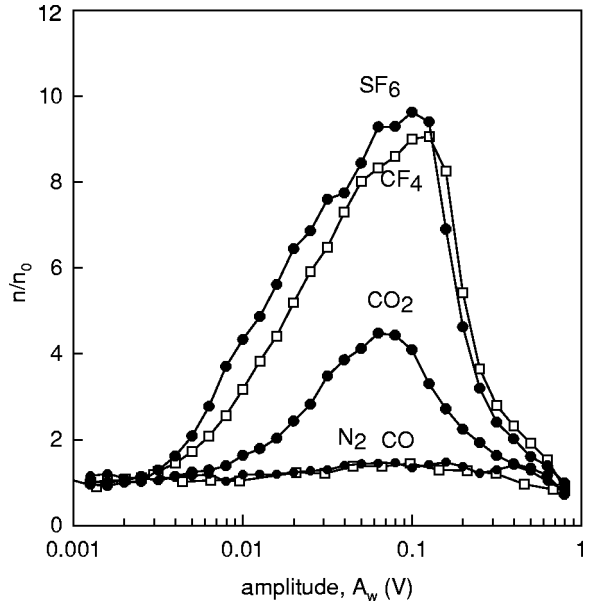

FIG. 7. Compression using cooling on various gases. $f_w = 2.5$ MHz, $P \sim 2 \times 10^{-8}$ torr.

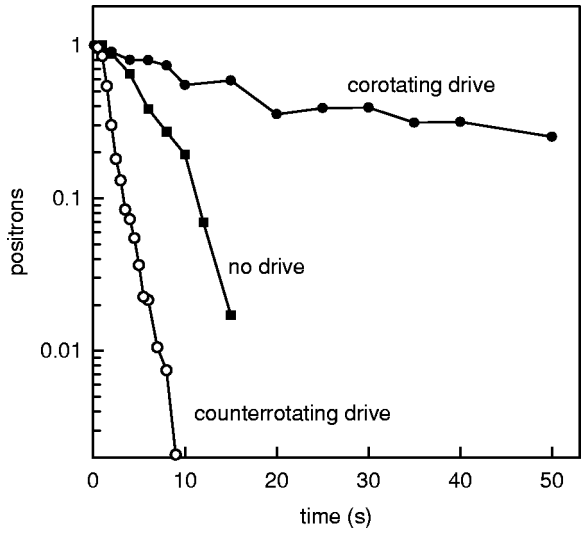

FIG. 8. Lifetime of a positron plasma with no rotating field applied, with the applied field rotating faster than the plasma rotation (''corotating drive''), and in the opposite direction (''counterrotating drive''). $f_w = 250$ kHz, $A_w = 330$ mV, $P = 1.8 \times 10^{-8}$ torr, CF_4.

this is a reasonable approximation to the compression rate $\dot{n}/n$, and the initial compression rate follows the predictions of linear theory, i.e., $\dot{n}/n \propto A_w^2$.[21] Thereafter, the compression rate begins to level off. Then at some critical amplitude it drops off as the amplitude is further increased.

Data for compression observed using different cooling gases are presented in Fig. 7. In general these gases exhibit similar amplitude dependences, but produce different compression rates, which are summarized in Table I. One surprising result is the small compression obtained using CO, which has a relatively high cooling rate. This shows that complicating factors play a role in the cooling process, probably reflecting details of the energy dependence of the positron-molecule cross sections. For example, CO has one of the largest vibrational quanta of the gases studied (see Table I), and so less effective cooling is expected below this energy.

In addition to providing compression, the rotating electric field provides the ability to improve positron confinement in cases where enhanced densities are not required. As shown in Fig. 8, application of a rotating field can reverse the outward transport that is a universal feature of non-neutral plasma confinement.[34] This figure also shows that plasma confinement is dramatically degraded by applying the rotating field opposite to the direction of plasma rotation. Another capability of the compression technique described here is the ability to confine plasmas even under conditions where the anomalous radial transport would otherwise lead to rapid plasma loss. Figure 9 shows positron lifetimes in the presence of the rotating field under conditions where the confining magnetic field is reduced following an initial compression phase of 5 s at 900 G. These data show that the positron lifetime is essentially independent of the magnetic field down to 100 G, even though at 100 G the positron confinement time is less than 1 s in the absence of the rotating field. In this case, the factor limiting the positron lifetime is annihilation on impurities in the vacuum system, rather than on the cooling gas.

IV. DISCUSSION

A. Coupling to the plasmas

The experiments described here were conducted in a different parameter range than those reported previously.[21,23] The previous experiments satisfied the condition $v_\phi \gg v_{\rm th}$, where $v_\phi \sim (\omega - m_\theta \omega_r)/k$ is the TG wave phase velocity and $v_{\rm th} = \sqrt{k_B T_p / m}$ is the positron thermal velocity. Under this condition, the TG modes were weakly damped. It can be shown that in this limit $R_p \gg \lambda_D$, and so the vacuum field only penetrates the plasma at frequencies near the resonant mode frequencies. In contrast, in the positron experiments

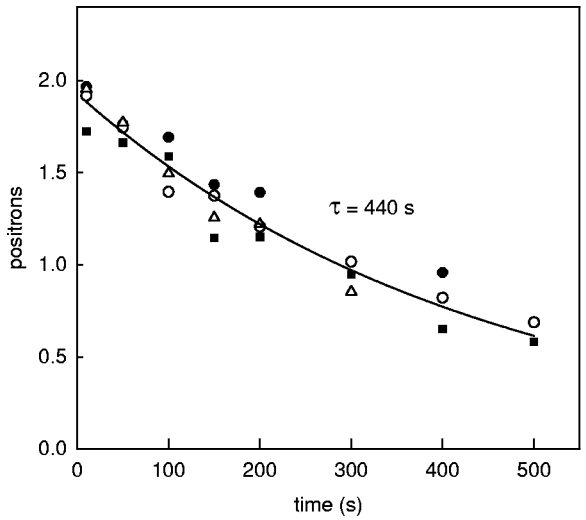

FIG. 9. Lifetime of a positron plasma in the presence of a rotating electric field at reduced magnetic field. (●) 900 G, (○) 400 G, (□) 200 G, (△) 100 G; $P = 3 \times 10^{-8}$ torr, $f_w = 2.5$ Mhz, $A_w = 30$ mV.

reported here, $v_\phi \sim v_{\rm th}$, in which case the TG modes are heavily damped as discussed below. In this same limit $R_p \sim 3\lambda_D$, and the rotating wall electric field can penetrate an appreciable fraction of the plasma even when no resonant mode is present (i.e., the Debye shielding is weak). Also, in this same limit, $f_w \sim v_{\rm th}/L$ and so the rotating wall field can couple directly to rotating bounce resonances of the plasma particles.[35,36]

The Landau damping rate γ of the TG modes scales as[23]

$$\gamma/\omega \sim -\frac{1}{2}\left(\frac{v_\phi}{v_{\rm th}}\right)^3 \exp\left[-\frac{1}{2}\left(\frac{v_\phi}{v_{\rm th}}\right)^2\right]. \quad (2)$$

For the earlier experiments where the plasma was much longer, and the phase velocity was therefore lower, $\gamma/\omega \sim -0.01$, while for the present experiment, $\gamma/\omega \sim -0.6$ at 0.025 eV and $\gamma/\omega \sim -0.2$ at $T_p = 0.1$ eV. Thus, in the wave picture, the much stronger damping in the present experiment can account qualitatively for both the higher compression rates (because of the more direct coupling between the applied electric field and particles), and for the nonresonant nature of the interaction, due to mode broadening. It also accounts for the failure to observe the mode directly on the pickup electrodes. The strong damping may also explain the scaling $\dot{n}/n \propto A_w^2$ observed here but not in previous experiments.

Thus, the results of the present experiment are consistent with those of previous rotating wall experiments.[21] However, since the TG modes are heavily damped in the parameter range studied here and do not evidence themselves in the dependence of the coupling on applied frequency, modeling the coupling as a direct interaction of the applied field with a rotating particle-bounce resonance may also be useful.

The coupling to the plasma in the limit of the experiments described here, in which R_p is not too much larger than λ_D, has the interesting consequence that compression begins at the outside of the plasma and then proceeds inward as the Debye shielding is reduced at the periphery of the plasma. This may explain the spatiotemporal dependence of the compression illustrated in Fig. 2, where plasma is swept inward from the broad initial distribution into a much narrower central peak. As mentioned above, the factors limiting the minimum radius of this central peak are not yet understood.

B. Potential applications

1. High-density positron plasmas

The compression technique described here provides a means for producing high density positron plasmas for a variety of uses. One such application is the production of cold antihydrogen for fundamental physics studies.[14] One of the most promising techniques that is currently being considered for antihydrogen production is the co-mingling of ultracold positrons and antiprotons in various configurations of multiple Penning traps.[14] One effort pursuing this goal at the European Center for Nuclear Research (CERN), the ATHENA collaboration,[37] is currently employing a high-efficiency positron accumulator similar to the one used in the experiments described here.[38] The use of plasma compression is currently being implemented on that device as a means of increasing positron densities and improving the ability to transport positrons from the accumulator to the trap where the antiproton and positron plasmas will be combined.[39] Other uses for high-density positron plasmas include study of electron–positron plasmas,[4] and the cooling of highly charged ions.[15]

2. Long-term positron plasma confinement

The data presented in Fig. 8 indicate that the rotating electric field can be used to eliminate positron plasma losses resulting from anomalous transport. Annihilation losses can also be eliminated by reducing impurities in the vacuum system. In particular hydrocarbon impurities, which have unusually large annihilation cross sections,[31] can be completely eliminated by storing the positrons in a cryogenic environment. This makes it possible to consider storing positrons for long periods. There are other cases in which a cryogenic environment would be cumbersome. For these applications, using well-designed traps to reduce anomalous losses, only minimal cooling gas would be required, thereby reducing annihilation losses. For example, using CF_4 at a pressure of 10^{-9} torr, the annihilation time would be about one day.

3. Brightness-enhanced positron beams

Positron plasmas in Penning traps have been used to create positron beams with low energy spreads.[8] Penning traps also offer novel approaches to the production of positron microbeams. Positron microbeams (i.e., with diameter <1 μm) can be used for a range of surface-scanning analytical tools for materials analysis. The factor limiting the spatial resolution that can be obtained for such a charged particle beam is the intrinsic brightness Ω^{-1}, where[40]

$$\Omega = D^2 \Delta E_\perp, \quad (3)$$

where $\Delta E_\perp$ is the perpendicular energy spread of the beam and D is its diameter. By Liouville's theorem, this quantity cannot be reduced using only conservative fields. The minimum beam diameter that can be obtained by focusing optics is $D_{\rm min} = \Theta^{-1}\sqrt{\Omega/E}$, where E is the beam energy and Θ is the convergence angle of the beam at the focus. Typically, $E_\perp = 1.5$ eV, $E = 5$ kV, and $D = 10$ mm, so $D_{\rm min} \sim D/20$. This limitation can be overcome using the technique of remoderation brightness enhancement,[41] in which the beam target is a material with a negative affinity for positrons, such as tungsten. A significant fraction of the incident positrons are reemitted after thermalizing with the solid, thus allowing them to be refocused to a smaller spot. By repeating this process several times, microbeams can be obtained. However, significant positron losses of 70–80% are incurred in each stage. In contrast, by compressing the plasma before beam extraction, similar brightness enhancement can be obtained at much higher efficiencies.

C. Future studies

The experiments described here represent a proof-of-principle demonstration of the ability of the rotating electric field technique to produce efficient positron plasma compres-

sion. Future studies will concentrate on developing a more complete understanding of the compression process to produce a more effective tool for use in a variety of applications such as those described above.

In particular, processes that limit the degree of compression that can be obtained will be further investigated. The diocotron mode that appears to develop during the compression can be eliminated by feedback stabilization. Anomalous transport processes can be reduced by careful alignment of the magnetic field with the axis of the trap.[42] Higher-order azimuthal modes such as $m_\theta = 2$ will be investigated and compared with the compression factors obtained from the $m_\theta = 1$ mode. The dependence of the compression process on plasma length will also be investigated, and more efficient cooling will be investigated using other gases and gas mixtures.

V. SUMMARY

We have made the first experimental demonstration of the compression of a magnetized positron plasma by applying a rotating electric field at frequencies well above the rotation frequency. An important result of these experiments is that for short plasmas, the reduced phase velocity of the TG modes leads to heavy damping. This in turn provides rapid and efficient compression over a broad range of frequencies.

A key element of these experiments was the implementation of buffer gas cooling using suitably chosen polyatomic gases. This has enabled good compression to be obtained at a relatively low magnetic field. This technique is likely to be useful in a variety of technological applications, including the production of brightness-enhanced positron beams.

ACKNOWLEDGMENTS

We wish to acknowledge helpful conversations with F. Anderegg, C. F. Driscoll, R. W. Gould, E. M. Hollmann, and T. M. O'Neil, and the assistance of S. J. Gilbert, E. Jerzewski, and J. Sullivan. This work is supported by the Office of Naval Research, Grants Nos. N00014-97-1-0366 and N00014-99-M-0317.

[1] W. E. Kauppila and T. S. Stein, Adv. At., Mol., Opt. Phys. **26**, 1 (1990).
[2] A. P. Mills, Jr., Science **218**, 335 (1982).
[3] P. J. Schultz and K. G. Lynn, Rev. Mod. Phys. **60**, 701 (1988).
[4] R. G. Greaves and C. M. Surko, Phys. Rev. Lett. **75**, 3846 (1995).
[5] L. D. Hulett, Jr., D. L. Donohue, J. Xu, T. A. Lewis, S. A. McLuckey, and G. L. Glish, Chem. Phys. Lett. **216**, 236 (1993).
[6] B. L. Brown and M. Leventhal, Phys. Rev. Lett. **57**, 1651 (1986).
[7] R. G. Greaves and C. M. Surko, Phys. Plasmas **4**, 1528 (1997).
[8] S. J. Gilbert, C. Kurz, R. G. Greaves, and C. M. Surko, Appl. Phys. Lett. **70**, 1944 (1997); A. S. Newbury, B. M. Jelenkovic, J. J. Bollinger, and D. J. Wineland, Phys. Rev. A **62**, 023405 (2000).
[9] D. J. Wineland, C. S. Weimer, and J. J. Bollinger, Hyperfine Interact. **76**, 115 (1993).
[10] R. G. Greaves and C. M. Surko, Phys. Rev. Lett. **85**, 1883 (2000).
[11] R. G. Greaves and C. M. Surko, in AIP Conference Proceedings No. 498, *Non-Neutral Plasma Physics III*, edited by J. J. Bollinger, R. L. Spencer, and R. C. Davidson (American Institute of Physics, Melville, New York, 1999), pp. 19–28.
[12] P. M. Platzman and J. P. Mills, Jr., Phys. Rev. B **49**, 454 (1994).
[13] C. M. Surko, M. Leventhal, W. S. Crane, A. Passner, and F. Wysocki, Rev. Sci. Instrum. **57**, 1862 (1986).
[14] M. Charlton, J. Eades, D. Horvath, R. J. Hughes, and C. Zimmermann, Phys. Rep. **241**, 65 (1994).
[15] D. A. Church, Phys. Scr. **46**, 278 (1992).
[16] W. M. Carreras, IEEE Trans. Plasma Sci. **25**, 1281 (1997).
[17] D. L. Eggleston, T. M. O'Neil, and J. H. Malmberg, Phys. Rev. Lett. **53**, 982 (1984); J. M. Kriesel and C. F. Driscoll, *ibid.* **85**, 2510 (2000); B. P. Cluggish and C. F. Driscoll, *ibid.* **81**, 4875 (1998).
[18] J. J. Bollinger and D. J. Wineland, Phys. Rev. Lett. **53**, 348 (1984); D. J. Heinzen, J. J. Bollinger, F. L. Moore, W. M. Itano, and D. J. Wineland, *ibid.* **66**, 2080 (1991).
[19] X. Huang, F. Anderegg, E. M. Hollmann, C. F. Driscoll, and T. M. O'Neil, Phys. Rev. Lett. **78**, 875 (1997).
[20] X. Huang, J. J. Bollinger, T. B. Mitchell, and W. M. Itano, Phys. Rev. Lett. **80**, 73 (1998).
[21] F. Anderegg, E. M. Hollmann, and C. F. Driscoll, Phys. Rev. Lett. **74**, 4213 (1995).
[22] R. W. Gould, in Ref. 11, pp. 170–175.
[23] E. Hollmann, F. Anderegg, and C. F. Driscoll, Phys. Plasmas **7**, 2776 (2000).
[24] C. S. Weimer, J. J. Bollinger, F. L. Moore, and D. J. Wineland, Phys. Rev. A **49**, 3842 (1994).
[25] T. B. Mitchell, Ph.D. thesis, University of California, San Diego, 1993.
[26] R. E. Pollock and F. Anderegg, AIP Conf. Proc. **331**, 139 (1995).
[27] T. I. Ichioka, H. Higaki, M. Hori, N. Oshima, K. Kuroki, A. Mohri, K. Komaki, and Y. Yamazaki, in Ref. 11, pp. 59–64.
[28] C. M. Surko, S. J. Gilbert, and R. G. Greaves, in Ref. 11, pp. 3–12.
[29] T. J. Murphy and C. M. Surko, Phys. Rev. A **46**, 5696 (1992).
[30] R. G. Greaves, M. D. Tinkle, and C. M. Surko, Phys. Plasmas **1**, 1439 (1994).
[31] K. Iwata, R. G. Greaves, T. J. Murphy, M. D. Tinkle, and C. M. Surko, Phys. Rev. A **51**, 473 (1995).
[32] S. J. Gilbert, R. G. Greaves, and C. M. Surko, Phys. Rev. Lett. **82**, 5032 (1999).
[33] D. L. Eggleston, C. F. Driscoll, B. R. Beck, A. W. Hyatt, and J. H. Malmberg, Phys. Fluids B **4**, 3432 (1992).
[34] J. H. Malmberg and C. F. Driscoll, Phys. Rev. Lett. **44**, 654 (1980).
[35] S. Crooks and T. M. O'Neil, Phys. Plasmas **2**, 355 (1995).
[36] D. L. Eggleston and T. O'Neil, Phys. Plasmas **6**, 2699 (1999).
[37] K. S. Fine, in Ref. 11, pp. 40–47.
[38] M. J. T. Collier, L.V. Jorgensen, O. I. Meshkov, D. P. van der Werf, and M. Charlton, in Ref. 11, pp. 13–18.
[39] M. Charlton (private communication).
[40] A. P. Mills, Jr., Exp. Methods Phys. Sci. **29A**, 39 (1995).
[41] A. P. Mills, Jr., Appl. Phys. **23**, 189 (1980).
[42] C. F. Driscoll, K. S. Fine, and J. H. Malmberg, Phys. Fluids **29**, 2015 (1986).